



# Extrusion–spheronisation of highly loaded 5-ASA multiparticulate dosage forms

G. Di Pretoro<sup>a</sup>, L. Zema<sup>a</sup>, A. Gazzaniga<sup>a</sup>, S.L. Rough<sup>b</sup>, D.I. Wilson<sup>b,\*</sup>

<sup>a</sup> Dipartimento di Scienze Farmaceutiche “P. Pratesi”, Via G. Colombo 71, 20133 Milano, Italy

<sup>b</sup> Department of Chemical Engineering and Biotechnology, New Museums Site, Pembroke Street, Cambridge CB2 3RA, United Kingdom

## ARTICLE INFO

### Article history:

Received 18 June 2010

Received in revised form

28 September 2010

Accepted 1 October 2010

Available online 8 October 2010

### Keywords:

5-Aminosalicylic acid

Ram extrusion

Liquid phase migration

Microcrystalline cellulose

Granulation

## ABSTRACT

The aim of the current work was to develop an extrusion–spheronisation (E–S) route to manufacture pellets with a high loading ( $\geq 90$  wt%) of 5-aminosalicylic acid (5-ASA). Ram extrusion studies, supported by centrifuge testing, were employed to investigate the effect of the chemical (acidity) and physical (particle size and shape) characteristics of 5-ASA on the ability of microcrystalline cellulose (MCC)-based pastes to retain water when subjected to pressure. Liquid phase migration (LPM) within the paste during the extrusion, and hence variation in water content of extrudates and reproducibility of the final E–S product, was generally observed. The extent of LPM was found to be related to both the drug loading and its physical properties, most notably the particle shape (needle-like). A reduction in particle size, combined with a change in the shape of the 5-ASA particles, allowed LPM to be reduced considerably or eliminated. The performance of colloidal grades of MCC (Avicel RC591 and CL611) as alternative extrusion aids to the standard Avicel PH101 was also investigated: these proved to be superior aids for the highly loaded 5-ASA pastes as their greater water retention capacity mitigated LPM. Combining these results yielded a route for manufacturing pellets with 5-ASA loading  $\geq 90$  wt%.

© 2010 Elsevier B.V. All rights reserved.

## 1. Introduction

### 1.1. 5-ASA treatment requirements

Crohn's disease (CD) and ulcerative colitis (UC) are chronic, episodic inflammatory conditions of the gastro-intestinal tract, which primarily affect the ileum and the colon, respectively (Cohen, 2006). The first-line drug therapy for mild to moderate acute exacerbations of CD and UC is, at present, based on 5-aminosalicylic acid (5-ASA, mesalamine). Since the anti-inflammatory action of 5-ASA is thought to be predominantly topical at the site of inflammation, oral modified-release delivery systems (e.g. enteric coated products) are generally employed to maximise drug delivery to the affected regions while minimising systemic absorption. 5-ASA is generally administered at the dosage regimen of 2.4 g/day, even though recent clinical trials have convincingly demonstrated that by doubling the standard dose of mesalamine, both safety and

efficacy and hence cost-effectiveness can be improved, with no increase in adverse events (Buckland and Bodger, 2008). However, most of the oral formulations currently available on the market are associated with a number of limitations, mainly a relatively low drug dosage (generally 500 mg 5-ASA/unit). Frequent daily dosing and a high number of tablets/capsules are therefore required for the treatment of CD and UC, at the expense of patient acceptability and adherence to therapy (Cervený et al., 2007).

To improve compliance, a high strength solid formulation containing more than 1 g 5-ASA/unit would be of interest, allowing once/twice daily administrations to be achieved. Multi-particulate dosage forms, based on high density pellets, have been sought as promising alternatives for the administration of 5-ASA, both for their biopharmaceutical (e.g. more even and predictable distribution and transportation in the gastro-intestinal tract) and technological (e.g. high drug loading) advantages (Bechgaard and Hagermann, 1978). Extrusion–spheronisation (E–S) was investigated as the manufacturing technique in the present work, as it offers the potential to produce highly loaded pellets (Gazzaniga et al., 1998). The E–S route has been used by several other workers to prepare granules containing 5-ASA where the focus has been on identifying extrusion aids (e.g. Goskonda et al., 1994; Chuong et al., 2008), as well as coating methods (Wei et al., 2010) to allow colonic delivery. The 5-ASA content of the pellets rarely exceeded 50 wt%. Both Hileman et al. (1993) and Rudolph et al. (2001) have reported pellets with high 5-ASA loadings, at 80 and 77.4 wt% d.b. levels, respectively, approaching that desired for a high strength dosage

**Abbreviations:** 5-ASA, 5-aminosalicylic acid; API, active pharmaceutical ingredient; B.E.T, Brunauer–Emmett–Teller; BM, ball-milled 5-ASA; CaSO<sub>4</sub>, calcium sulphate dihydrate; CD, Crohn's disease; DSC, differential scanning calorimetry; E–S, extrusion–spheronisation; HD, high density grade of 5-ASA; JM, jet-milled 5-ASA; LPM, liquid phase migration; MCC, microcrystalline cellulose; NaCMC, sodium carboxymethyl cellulose; PXRD, powder X-ray diffraction; UC, ulcerative colitis; uM, un-milled 5-ASA.

\* Corresponding author. Tel.: +44 1223 334777; fax: +44 1223 334796.

E-mail address: [diw11@cam.ac.uk](mailto:diw11@cam.ac.uk) (D.I. Wilson).

### Nomenclature

$A$	projected area of particle ( $\text{m}^2$ )
$d_{10}, d_{50}, d_{90}$	particle size (m)
$D$	die land diameter (m)
$L$	die land length (m)
$p$	projected perimeter of particle (m)
$P_c$	centrifugal pressure (Pa)
$P_{ex}$	extrusion pressure (Pa)
$r_{in}, r_{out}$	radial distances (m)
$V_{ram}$	ram velocity ( $\text{m s}^{-1}$ )
$\rho$	liquid phase density ( $\text{kg m}^{-3}$ )
$\omega$	angular velocity ( $\text{rad s}^{-1}$ )

form. Higher 5-ASA loadings, approaching the 90 wt% sought in this study, have not been achieved, to the authors' knowledge.

### 1.2. Extrusion–spheronisation

Extrusion–spheronisation is a multi-stage mechanical process, in which a wet mass is forced through a die/screen and afterwards shaped into small spherical/near-spherical granules. The liquid phase (generally water) provides interparticle cohesion, lubricates particle contacts, promotes wall slip and can also bear some of the stress generated during the forming process. However, the pressure exerted on the liquid phase during extrusion can cause it to move faster with respect to the particulate network, giving rise to variation in the liquid content of the paste within the barrel and hence the extrudates. The redistribution of the liquid phase within the solid matrix is known as liquid phase migration (LPM) or 'dewatering' (Mascia et al., 2006). The occurrence of LPM phenomena is affected by the amount and the viscosity of the liquid phase, solids packing and structure, along with process parameters (e.g. extrusion velocity and die/screen geometry) (Bains et al., 1991).

The physical and chemical properties of the active pharmaceutical ingredient (API) are important in paste formulation: the solubility of the API in the liquid phase, its particle size characteristics and packing behaviour can affect the amount of liquid necessary to obtain a wet mass with the required 'plasticity' (Vervaeke et al., 1995). Hagsten et al. (2008) identified particle size, specific surface area and packing behaviour to be key factors affecting the variation in processability (in terms of the amount of liquid required for extrusion) of 131 batches of 5-ASA processed by E–S.

Particle size and particle morphology also have a significant influence on the rheology of the wet powder masses and the occurrence of LPM. Fielden et al. (1992) investigated the influence of lactose size distribution on extrusion behaviour and pellet characteristics of lactose/water pastes. Increasing the particle size resulted in high extrusion pressures and promoted LPM. Particle packing and solids matrix strength are both controlled by particle shape and volume fraction. The porosity and pore size distribution in the wet mass, and thereby the permeability of (and likelihood of LPM within) the extrudate, are also determined by particle shape and volume fraction. The rheological behaviour of suspensions is also sensitive to particle shape, with the intrinsic viscosity of particles in the Krieger–Dougherty equation known to increase as the shape becomes less spherical (Krieger and Dougherty, 1959). 5-ASA crystals are normally needle-like: Kraeger et al. (2004) studied the influence of size and shape of another needle-shaped API, paracetamol, on dry powder properties and pelletisation, but the impact of particle shape on extrusion–spheronisation has not, to our knowledge, been considered in depth.

### 1.3. E–S aids

Since the active ingredients do not generally have either lubricant or plasticising properties, an extrusion spheronisation aid, namely an excipient able to provide mechanical structure and rheological stability, is usually required. Microcrystalline cellulose (MCC) is a well established E–S aid whose interaction with water is primarily physical rather than chemical. MCC absorbs water and confers the appropriate degree of plasticity to the bulk, as well as controlling the movement of water through the wet powder mass during extrusion. Fielden et al. (1988) suggested, on the basis of thermal studies, that MCC could be described as a 'molecular sponge': it is capable of not only physically retaining a large quantity of water within its fibrous network, but also of allowing its removal to take place by evaporation and when subjected to pressure.

Not all APIs can be processed with the standard grade of MCC (e.g. Avicel PH101), particularly when high loadings (i.e. above 70 wt%) are required. The inability of Avicel PH101 either to allow the extrusion (Tomer et al., 2001) or the spheronisation (Tomer et al., 2002) of highly loaded formulations seems to be related to its limited water-retention capacity when subjected to pressure. Podczek and Knight (2006) reported that the inability of Avicel PH101 to support E–S of pastes containing 80 wt% of a water-insoluble drug (ibuprofen) was associated with the migration of water within the formulation during the extrusion stage.

Modified MCC grades, co-processed with varying amounts of sodium carboxymethyl cellulose (NaCMC) are able to retain higher quantities of water than the standard Avicel PH101 and have therefore been proposed as alternative E–S aids for high solids loadings. These modified MCC grades (e.g. Avicel RC591 and CL611) were identified by several workers, e.g. O'Connor et al. (1984) and Hileman et al. (1993), as promising aids in the extrusion of high solids loading formulations, improving extrusion performance and surface quality of the extrudates formed. This behaviour was found to be related to their ability to restrict migration of water in the wet mass when subjected to pressure (Podczek et al., 2007). However, the improved quality of surface extrudates was always obtained at the expense of rigidity of the extrudates, which led to difficulties in spheronisation. In fact, good quality extrudate does not always imply its suitability for spheronisation, as demonstrated by Rough and Wilson (2005).

The aim of the current work was to assess the feasibility of an E–S route for the manufacture of pellets with high 5-ASA loading (i.e. >80 wt%). Initial attempts to produce pellets in a radial screen extruder (Nica System, model E140), using Avicel PH101 as the E–S aid and water as the liquid binder, were undertaken. A screening design of experiments, aiming to identify the most critical process and formulation parameters for the obtainment of pellets with desirable properties (e.g. high drug content, low friability, high density and sphericity), was determined. However, variability in extrudate water content coupled with a lack of reproducibility of pellet properties was generally observed, in such a way that the experimental design was invalidated. In particular, the optimal amount of water necessary to achieve both a plastic mass suitable for extrusion, and extrudates with appropriate characteristics for spheronisation, could not be identified. A likely hypothesis to explain the variability in extrudate water content could be that pastes undergo dewatering when subjected to high pressures, i.e. during the extrusion process. A systematic study was therefore performed in a ram extruder apparatus to investigate the influence of both solid phase components, namely the active ingredient (physical and chemical characteristics) and the E–S aid, on the rheological properties of highly loaded 5-ASA pastes undergoing extrusion.

## 2. Materials and methods

### 2.1. Materials

5-Aminosalicylic acid (5-ASA, mesalamine) (Erregierre S.p.A., Bergamo, Italy) was used both as received from the supplier (unmilled, labelled uM) and after micronisation. Calcium sulphate dihydrate ( $\text{CaSO}_4 \cdot 2\text{H}_2\text{O}$ , labelled  $\text{CaSO}_4$ ) (Fisher Scientific Inc., Pittsburgh, PA, USA) and a high density grade of 5-ASA (labelled 5-ASA HD) (Farchemia S.p.A., Treviglio, Italy) were chosen as reference materials to investigate the influence of prolate (needle-like) particles on the extrusion process. The standard Avicel PH101 grade of microcrystalline cellulose (MCC) (IMCD S.p.A., San Donato Milanese, Italy) was used as the primary extrusion–spheronisation aid. Two modified grades of MCC co-processed with sodium carboxymethyl cellulose (NaCMC), namely Avicel RC591 (12 wt% NaCMC) and Avicel CL611 (15 wt% NaCMC), were evaluated as alternatives to Avicel PH101. Reverse osmosis water was used as the binder for paste preparation.

### 2.2. Methods

#### 2.2.1. Micronisation

Two batches of micronised 5-ASA were obtained by milling uM in different equipment. The BM batch was prepared in a planetary ball mill (Pulverisette 7, Fritsch, Germany); the grinding process was performed in a 45 mL stainless steel grinding bowl containing 14 stainless steel balls (20 mm diameter), for 12 h at 250 rpm. A standard Teflon seal was positioned between the lid of the grinding bowl and the bowl itself. The powder-to-ball weight ratio was 1/35. The JM batch was kindly provided by IMS Micronizzazioni S.p.A. (Milano, Italy). The batch was produced by air-jet milling (Chrispro® Jet-Mill, Micro-Macinazione S.A., Molinazzo di Monteggio, Switzerland). The mill had a spiral chamber of 300 mm diameter. The milling gas was air, injected through 8 nozzles at 8 bar. The starting material was charged ( $700\text{--}750\text{ g min}^{-1}$ ) through a venturi feeder, using a pressure of 8 bar.

#### 2.2.2. Powder characterisation

**2.2.2.1. Powder X-ray diffraction.** Powder X-ray diffraction (PXRD) was performed on a Philips PW1050/25 diffractometer (Philips Analytical Inc., Natick, MA, USA) using  $\text{Cu-K}\alpha$  radiation ( $\lambda = 1.54 \text{ \AA}$ ) generated with 30 kV and 15 mA. Samples were packed in the same aluminum sample holder to promote reproducibility of conditions, taking care also to minimize preferred orientation effects. The operating conditions were as follows: scan speed  $0.5^\circ \text{ min}^{-1}$   $2\theta$ ; step size  $0.02^\circ 2\theta$ ; range  $5 \leq 2\theta \leq 35^\circ$ .

**2.2.2.2. Thermal analysis.** Differential scanning calorimetry (DSC) was performed on a DSC2010 calorimeter (TA Instruments, New Castle, DE, USA), between ambient and  $350^\circ\text{C}$ , under nitrogen purging at  $70\text{ mL min}^{-1}$ . DSC runs were performed on 2–3 mg samples in non-hermetically sealed aluminum pans at a scanning rate of  $10\text{ K min}^{-1}$ . Data reported are the average of at least 3 determinations.

**2.2.2.3. Solid, bulk and tapped densities.** The solid density of the three batches of 5-ASA (uM, JM and BM) was evaluated using a Micromeritics AccuPyc 1330 helium pycnometer (Norcross, GA, USA). The gas pressure was set to be 0.087 psia with a purging time of  $\sim 15$  min. Samples of 0.3–0.5 g were analysed in a controlled environment ( $26.1^\circ\text{C}$ , relative humidity 50%). All the analyses were conducted in triplicate. For the bulk and tapped densities, a sample mass of about 50 g was poured into a 250 mL glass cylinder mounted on an automated tap density tester (Stampfvolumeter STAV 2003, Engelsmann A.G., Ludwigshafen, Germany). The volume of powder

was determined after zero and 1250 taps, and the bulk and tapped densities were calculated as the ratio of the mass to the corresponding volumes, respectively. The results presented are the mean of three replicates.

**2.2.2.4. BET surface measurements.** Surface area determination was performed by means of a SA3100 Surface Area Analyzer (Beckman Coulter, UK) according to the BET method using  $\text{N}_2$  as adsorbate gas (USP 32 *Physical Test. Specific Surface Area. Volumetric Method*). Prior to surface area measurements, the samples (approximately 2 g) were degassed at  $90^\circ\text{C}$  under vacuum (0.4 Pa) for 1 h to remove physically adsorbed gases (water vapour). The measurement was carried out in triplicate.

**2.2.2.5. Particle size and shape.** Particle size characterisation was performed using a laser light scattering and an automated particle imaging apparatus. The laser scattering device was a Coulter LS 230 (Beckman Coulter Inc., Fullerton, CA, USA) equipped with variable speed, microvolume and dry powder modules. Lorentz–Mie theory (diffraction–diffusion) was used as the optical model. The refractive indices of 5-ASA and  $\text{CaSO}_4$  were taken as 1.691 and 1.521, respectively. Isopropyl alcohol (refractive index 1.377) and pure sunflower oil (refractive index 1.473) were used as suspending agents for 5-ASA and  $\text{CaSO}_4$ , respectively. Powder samples were sonicated prior to analysis to break up potential aggregates. Data collected are reported in terms of volume-based relative size distribution.

The particle imaging device (Morphologi® G3, Malvern Instruments Ltd, Worcestershire, UK) was able to determine both particle size and shape. The machine featured a Nikon CFI 60 Brightfield/Darkfield optical system and a 1/1.8 in. global shutter progressive scan CCD camera (5 megapixels). Powder samples ( $3\text{ }\mu\text{m}^3$ ) were dispersed using the integrated sample dispersion unit, via an instantaneous pulse of compressed air (range: 0.8–2.5 bar depending on the particle size of the powders). Image analyses were performed at  $20\times$  and  $50\times$  magnification, according to a standard operating procedure. Particle dimensions were quantified in terms of volume-based size distributions. Particle shape was quantified in terms of circularity (calculated as  $4\pi A/p^2$ , where  $A$  is the projected area and  $p$  the projected perimeter of the particle) and aspect ratio (defined as minor axis/major axis). At least 60,000 particles were analysed. Two-dimensional micrographs were also collected.

#### 2.2.3. Paste preparation

Dry powders (200–300 g) were placed in a planetary mixer (Kenwood KM 200, Southampton, UK) and different amounts of liquid binder slowly poured onto the powder surface. Granulation was performed at a constant speed of 25 rpm for 10 min. The process was occasionally interrupted to scrape off the material adhering to the wall of the bowl and the mixing blade. Mixtures of 5-ASA batches and MCC were dry blended for 5 min prior to liquid addition. Pastes were stored for 24 h in airtight containers prior to extrusion to allow the water to equilibrate throughout the mixture. All experiments were performed at room temperature in an air-conditioned laboratory ( $21 \pm 3^\circ\text{C}$ , humidity  $35 \pm 5\%$ ).

#### 2.2.4. Centrifuge testing

The centrifuge used was an MSE minor ‘s’ (Meadowrose Scientific Ltd., Oxfordshire, UK) operating over the range of 500–4600 rpm. Paste samples were filled into cylindrical copper containers (22 mm internal diameter (i.d.), 85 mm height), featuring a punctured base (several holes, i.d. 2 mm), to a sample height of 50 mm. A filter paper (1  $\mu\text{m}$  pore size) was placed at the bottom of the container to prevent loss of solid through the holes during centrifugation. The container was located in a stainless steel holder

attached at the end of a shaft rotating around the centrifuge axis. Samples were weighed before and after centrifugation performed at constant rotational speed for 60 and 120 min; trials were performed at different rotational speeds. All the experiments were carried out at room temperature ( $21 \pm 1^\circ\text{C}$ ) and environmental relative humidity ( $45 \pm 5\%$ ) to reduce the effects of water evaporation.

The centrifugal pressure,  $P_c$ , was calculated by the following relationship (Hassler and Brunner, 1945):

$$P_c = 0.5\rho\omega^2(r_{\text{out}}^2 - r_{\text{in}}^2) \quad (1)$$

where  $\rho$  is the liquid phase density,  $\omega$  the angular velocity, and  $r_{\text{in}}$  (75 mm) and  $r_{\text{out}}$  (85 mm) are the radial distances from the centrifuge axis to the inner and outer faces of the sample, respectively. Final water content (and drainage) was quantified in terms of the water/MCC mass ratio, calculated as the mass of liquid retained by the sample after being centrifuged and the amount of MCC present in the sample.

### 2.2.5. Extrusion–spheronisation

Extrusion testing was performed in a computer-controlled ram extruder (Zwick/Roell, Zwick Testing Machines Limited, Leominster, UK). The apparatus consisted of a 25 mm i.d. barrel, a ram attached to the cross-head of the strain frame and a load cell that measured the applied force and the ram displacement, as described by Rough et al. (2000). Various concentric cylindrical square-entry dies with different die land lengths ( $L$ ) and diameters ( $D$ ) were used. All surfaces in contact with the paste were stainless steel except the piston, which featured a Teflon seal. The barrel was filled with approximately 80 g of paste; to ensure uniform compaction a pre-load (range: 1–2 kN) was applied. Pastes were extruded at a constant ram velocity ( $V_{\text{ram}}$ ) in the  $0.1$ – $10\text{ mm s}^{-1}$  range. Extrudates were spheronised in a 120 mm diameter cross-hatch plate spheroniser (Caleva, Sturminster Newton, Dorset, UK), at a constant speed of 1600 rpm. Pellets were dried in a vacuum oven at  $40^\circ\text{C}$  for 24 h.

## 3. Results and discussion

### 3.1. Ram extrusion study of Avicel PH101-based 5-ASA pastes

Extrusion pressure ( $P_{\text{ex}}$ )–ram displacement profiles for Avicel PH101-based pastes containing increasing amounts of uM were compared at different experimental conditions (die length and diameter, ram velocity and paste water content). A steady increase in  $P_{\text{ex}}$  during the extrusion was generally observed for all the formulations tested. The phenomenon was more evident at lower extrusion velocities (data not shown). LPM is often manifested as a divergence from the expected steady-state  $P_{\text{ex}}$  value, and it was most noticeable with single-holed capillary dies having a high  $L/D$  ratio and/or at relatively low ram (and hence extrusion) velocities. The effect of die geometry and extrusion velocity on LPM has been discussed elsewhere (e.g. Rough et al., 2002). In order to mitigate the effects of LPM caused by relatively low ram velocities, a square-entry multi-holed die (6 notionally identical holes,  $D = 1\text{ mm}$ ,  $L = 4\text{ mm}$ , evenly spaced in a ring, radial distance from the die centre 7.5 mm) was employed for the majority of the tests, so that relatively low extrusion velocities could be attained with correspondingly high ram velocities (the ram velocity being directly proportional to the number of die holes multiplied by the extrusion velocity).

The paste water content was chosen to be just sufficient to give a plastic mass and suitable paste rheological properties for extrusion. The water/Avicel PH101 ratio was varied systematically to evaluate the influence of moisture content on the E–S process. The 1.2:1 water/Avicel PH101 ratio (by mass) was identified, by centrifugation testing (see Section 3.4.1), as the lower liquid limit for a

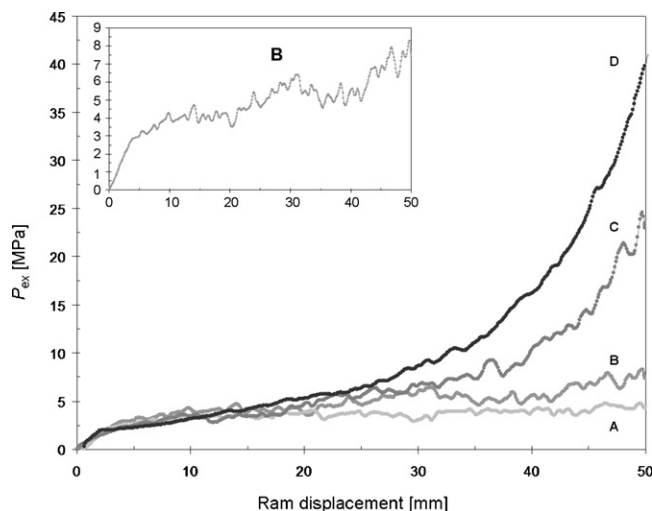


**Fig. 1.** Extrusion profiles for Avicel PH101-based pastes containing (A) 10 wt%, (B) 20 wt%, (C) 30 wt% and (D) 50 wt% uM at  $V_{\text{ram}} = 1\text{ mm s}^{-1}$ , 6-holed die ( $D = 1\text{ mm}$ ,  $L = 4\text{ mm}$ ). Water:Avicel PH101 ratio = 1.2:1. Inset shows a magnification of profile B, indicating how LPM occurred even at low drug loadings.

plastic mass. An increase in the liquid content resulted in over-wet pastes, whereas a decrease yielded dry and stiff pastes that were unsuitable for extrusion.

By way of example, Fig. 1 shows the  $P_{\text{ex}}$ –ram displacement profiles of pastes containing uM at 10–50 wt% of the total solids, performed using the multi-holed die at a ram velocity of  $1\text{ mm s}^{-1}$  (corresponding to an extrusion velocity of  $104\text{ mm s}^{-1}$ ). For a given ram displacement,  $P_{\text{ex}}$  increases as the uM content increases, indicating that LPM was related to the uM loading in the paste. For comparison, extrusion of a water/Avicel only paste under these conditions gave a steady  $P_{\text{ex}}$  value of  $\sim 2\text{ MPa}$ . Above 50 wt% 5-ASA, substantial dewatering of the paste was observed, resulting in  $P_{\text{ex}}$  approaching the mechanical limit of the apparatus. A systematic study of 5-ASA loading with Avicel PH101 was therefore not possible as LPM effects dominated the extrusion behaviour.

The increase in LPM with 5-ASA loading could arise from either a physical or a chemical interaction of the API with Avicel PH101, thereby modifying the rheological properties of the final wet mass. 5-ASA is sparingly soluble in water and therefore is present as ‘hard’ particles within a ‘soft’ MCC matrix. At high drug loadings, 5-ASA could affect the ability of the Avicel PH101 to support extrusion. Alternately, as 5-ASA solution is acidic, the liquid holding capacity of the MCC could be modified.

The effect of the physical properties of 5-ASA, specifically the particle size and shape, and the potential influence of 5-ASA acidity on the behaviour of Avicel PH101-based pastes during extrusion were therefore investigated. In addition, the performance of two colloidal grades of MCC, namely Avicel RC591 and CL611, as E–S aids was compared to that of the standard Avicel PH101.

### 3.2. Influence of 5-ASA acidity

5-ASA is a zwitterionic drug, with  $\text{pK}_a$  values of 6.0, 3.0 and 13.9 corresponding to the  $\text{NH}_3^+$ ,  $\text{COOH}$  and  $\text{OH}$  groups, respectively (Allgayer et al., 1985). Since water was used as the liquid binder, 5-ASA could alter the pH of the mobile phase, thereby influencing the ability of the MCC to work as a molecular sponge. The liquid retention ability of Avicel PH101-based pastes was therefore assessed using RO water and saturated aqueous solutions of 5-ASA ( $\text{pH} = 4 \pm 0.05$ ,  $\sim 0.9\text{ g L}^{-1}$ ) as the wetting/binding agent. Data were collected from centrifuge and ram extrusion testing, performed on different pastes prepared with 45–65 wt% liquid phase. The results



**Table 1**  
Particle size data for 5-ASA batches.

	Volume basis	uM		JM		BM	
		Laser scattering	Automated microscope	Laser scattering	Automated microscope	Laser scattering	Automated microscope
Particle size parameter/ $\mu\text{m}$	$d_{10}$	4.8	9.6	2.4	7.4	0.12	8.5
	$d_{50}$	41.4	20.3	5.6	13.0	1.6	28.5
	$d_{90}$	453	117	14.3	28.5	4.0	59.7

from these tests did not show any significant differences between water and 5-ASA saturated solution as binder, thereby indicating negligible influence of 5-ASA acidity on MCC liquid retention and flow behaviour.

### 3.3. Influence of 5-ASA physical properties

In order to assess the effect of 5-ASA physical properties on the extrusion behaviour of Avicel PH101-based pastes, three batches of 5-ASA, having different particle size and shape characteristics and hence different bulk properties, were investigated. The 5-ASA batches were:

- (i) the material as received by the supplier, labelled uM;
- (ii) the material in (i) after being subjected to jet milling, labelled JM;
- (iii) the material in (i) after being subjected to ball milling, labelled BM.

Their particle size characteristics, measured by the laser scattering and automated microscope devices, are summarised in Table 1. Both milling procedures reduced the particle dimensions, as indicated by the  $d_{10}$ ,  $d_{50}$  and  $d_{90}$  values. Divergences between the two measuring techniques are evident: the laser scattering data indicate that the BM material has a smaller particle size and narrower size distribution than JM whereas the opposite trend is indicated by the microscopy results. These differences were not surprising, as the devices employ different techniques and needle-like particle shapes further complicate the analysis. The micrographs in Fig. 2 confirm the difference in size and shape between the different batches. The BM particles are smaller than those in the other batches, while the JM particles are still needle-like although with a smaller aspect ratio than uM.

The reliability of laser scattering for aspherical particles has been discussed by Latimer et al. (1978). In contrast, the microscope system captures two-dimensional images of the particles and calculates particle size and shape parameters from these. Aggregates of BM particles are evident in Fig. 2(c), which are likely due to uneven dispersion of the sample in the microscopy preparation step: these aggregates will skew the particle size analysis data away from the trends indicated by the micrographs and laser sizing results. The need for careful sample preparation is evident.

The particle shape distribution data in Fig. 3 quantify the differences evident in the 2D micrographs in Fig. 2. Other measures of shape could be readily calculated from the data sets: we chose to report circularity and aspect ratio as these capture the key results of milling. Ball milling increases the circularity of the 5-ASA from the broad distribution centred at 0.45 obtained for both uM and JM materials to a narrower distribution with a mean of 0.85. The aspect ratio distributions in Fig. 3(b) reflect the above differences between uM and BM. Fig. 3(a) also indicates that jet milling gives a noticeably broader distribution in circularity.

Milling therefore changed the particle dimensions and shape. The impact on the powder handling properties is summarised in Table 2. The solid density values are very similar, as expected. In comparison with the uM values, the data indicate that the

jet milling process did not modify either the bulk or the tapped densities of the 5-ASA powder considerably. The tapped density decreases slightly after jet milling, probably due to electrostatic attractive forces becoming stronger as the particle dimensions

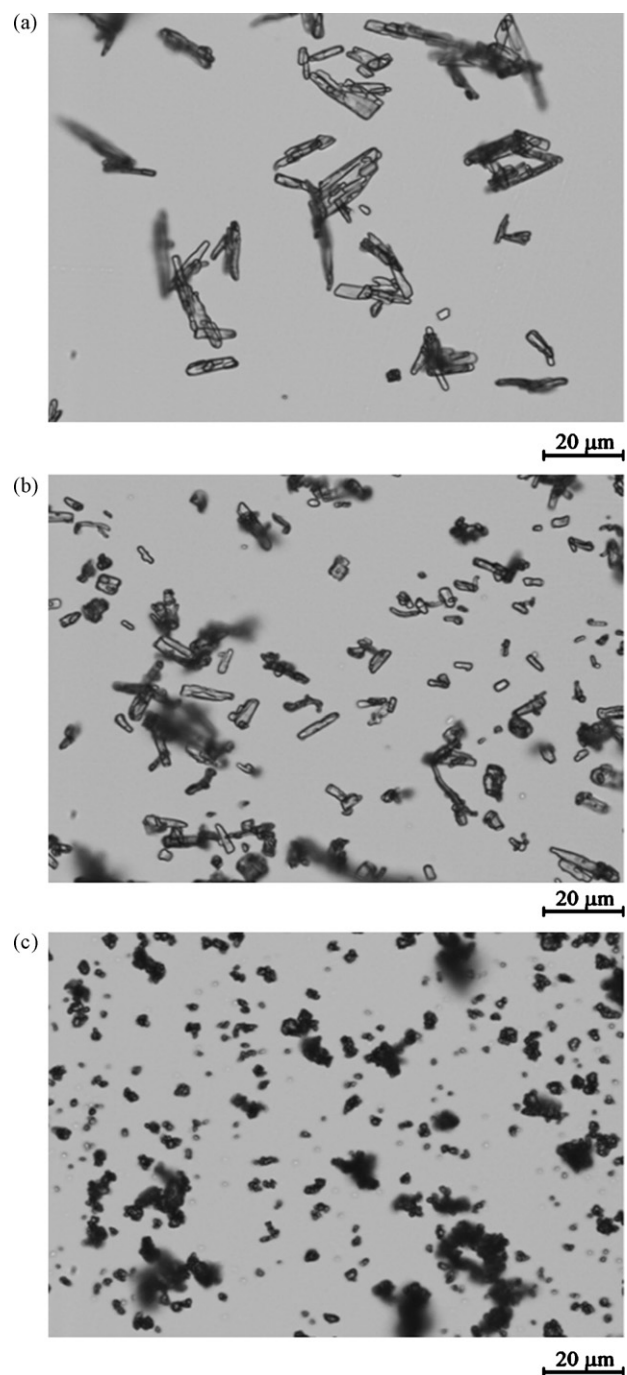


**Fig. 2.** Micrographs of (a) uM, (b) JM and (c) BM batches of 5-ASA (magnification 50 $\times$ ).

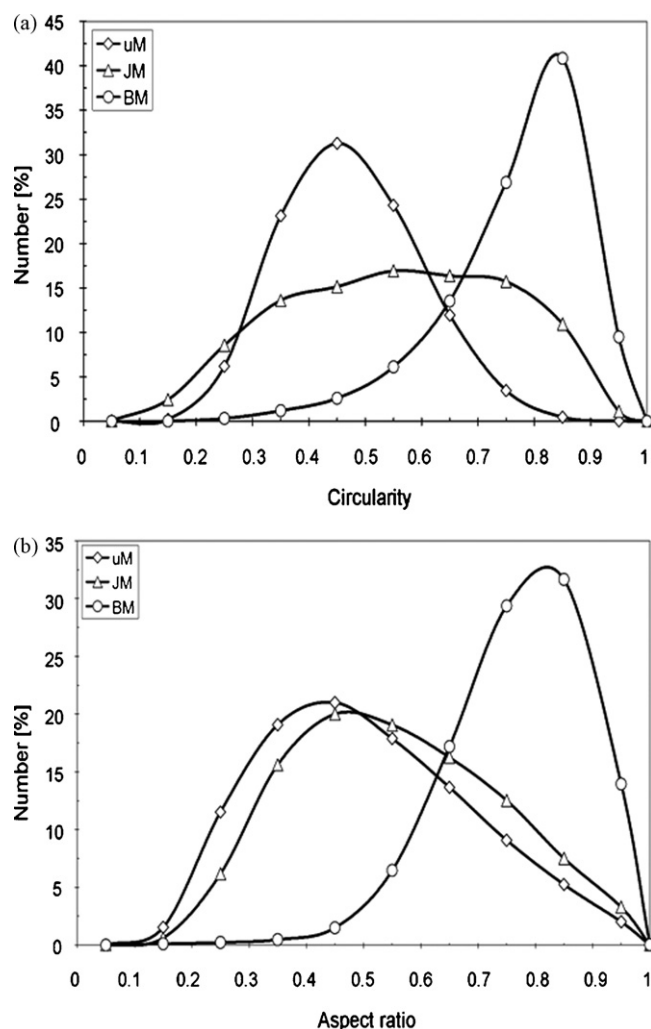


**Fig. 3.** Shape parameters for uM, JM and BM batches of 5-ASA obtained from image analysis: (a) circularity and (b) aspect ratio.

decrease, increasing particle aggregation and thereby leading to poorer packing ability. In contrast, the bulk and tapped density values for BM are about 50% and 60% higher, respectively, than the uM values. The differences in packing between JM and BM are consistent with the change in particle morphology and dimensions. The specific surface area (BET) results confirm the reduction in particle size upon milling. The trend supports the laser scattering sizing results (Table 1) in that the BM surface area is greater than that of the JM.

Modification of the solid state on milling was evaluated by PXRD and DSC. Fig. 4 shows similar PXRD patterns for the three materials. The peak angular positions are in excellent agreement, indicating that milling did not affect the crystalline form of 5-ASA. Small differences in the peak relative intensities are attributed to preferred orientation effects; this is consistent with the differing morphology of the 5-ASA crystals, being predominantly prolate for

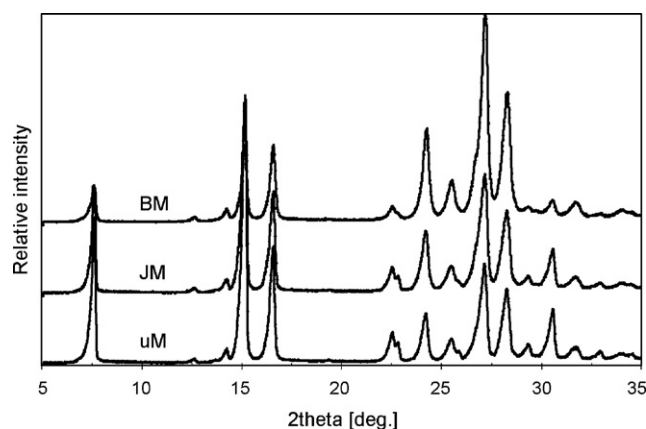


**Fig. 4.** X-ray diffraction patterns for uM, JM and BM batches of 5-ASA. Profile base-lines are shifted for clarity.

the uM and the JM batches, and more pseudo-spherical for BM, as discussed above. Similarly, thermograms of all samples showed a single endothermic melting event at approximately 280 °C with a comparable associated enthalpy (about 980 J g<sup>-1</sup>).

### 3.3.1. Ram extrusion study

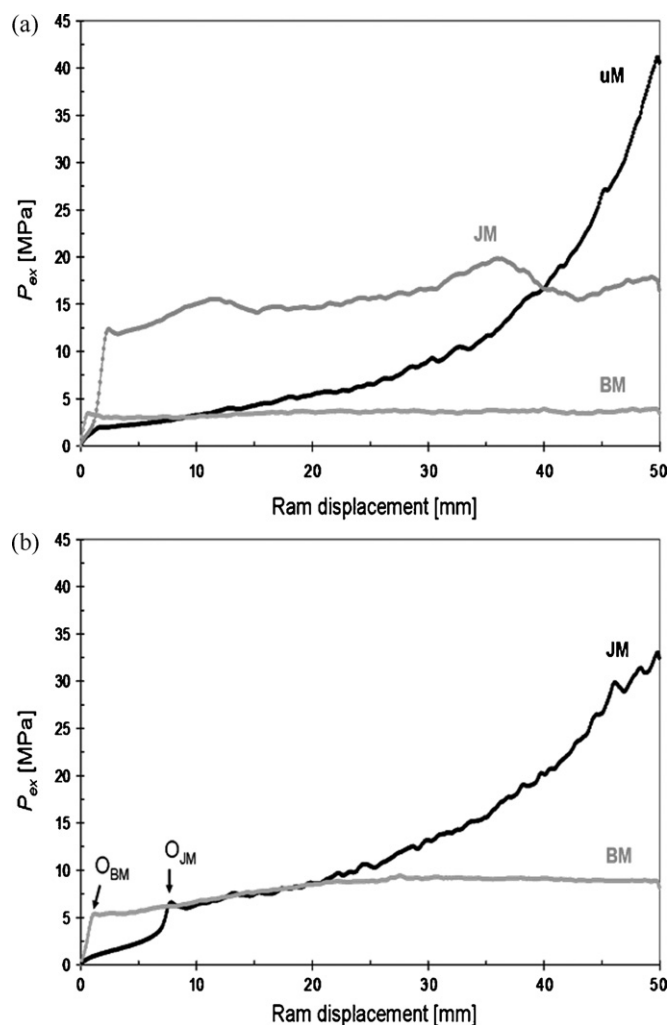
The effect of 5-ASA particle size and morphology on Avicel PH101 based pastes undergoing extrusion was investigated at varying experimental conditions of die length and diameter. Fig. 5 presents some of the extrusion pressure–ram displacement profiles obtained for (a) 50 wt% and (b) 90 wt% loaded 5-ASA pastes, performed at  $V_{\text{ram}} = 1 \text{ mm s}^{-1}$  using a 6-holed square-entry die ( $D = 1 \text{ mm}$ ,  $L = 4 \text{ mm}$ ).

Fig. 5(a) compares the ram extrusion profiles for 50 wt% loaded 5-ASA pastes. The 50 wt% loaded uM paste starts extruding at an initial  $P_{\text{ex}}$  value of ~2 MPa, but soon after the onset of the extrusion  $P_{\text{ex}}$  steadily increases, reaching a final value of ~41 MPa. This phenomenon is consistent with significant dewatering occurring during extrusion, leading to an over-wet initial mass, requiring a smaller stress to start flowing. Subsequent portions of paste being extruded are consequently drier, and higher pressures are hence required to maintain flow. As discussed in Section 3.1, LPM increases with increasing drug loading; at 90 wt% loading, the uM paste was unable to be extruded since severe dewatering occurred, yielding a dry immovable plug in the barrel.

50 wt% loaded JM and BM pastes start extruding at slightly higher  $P_{\text{ex}}$  values than uM, namely 13 and 4 MPa, respectively; however, unlike uM, the extrusion pressure reaches a steady state instead of progressively increasing, indicating that dewatering is minimal. Hence, a decrease in 5-ASA particle size improves the flow characteristics of wet powder masses and allows LPM to be considerably reduced or eliminated. This is particularly important when the longest particle dimension approaches the size of the die diameter. However, differences between JM and BM data are observed; the extrusion profiles for BM pastes are smooth and continuous, unlike JM which shows more fluctuation. The more jagged appearance of the  $P_{\text{ex}}$  profiles for the JM paste could be due to the greater tendency of the material to stick-slip at the die wall. The differ-

**Table 2**  
Density values ( $\pm$ s.d.) and specific surface area for 5-ASA batches.

Batch	Density/g cm <sup>-3</sup>			Specific surface area/m <sup>2</sup> g <sup>-1</sup>
	Solid	Bulk	Tapped	
uM	1.530 $\pm$ 0.001	0.240 $\pm$ 0.002	0.410 $\pm$ 0.008	1.94 $\pm$ 0.025
JM	1.517 $\pm$ 0.001	0.245 $\pm$ 0.005	0.344 $\pm$ 0.004	2.65 $\pm$ 0.022
BM	1.515 $\pm$ 0.001	0.480 $\pm$ 0.002	0.670 $\pm$ 0.003	5.89 $\pm$ 0.043



**Fig. 5.** Extrusion profiles for Avicel PH101/5-ASA (uM, BM and JM) pastes at  $V_{ram} = 1 \text{ mm s}^{-1}$ , 6-holed die ( $D = 1 \text{ mm}$ ,  $L = 4 \text{ mm}$ ). 5-ASA loading: (a) 50 and (b) 90 wt%. Points labelled  $O_{JM}$  and  $O_{BM}$  in (b) represent onset of flow for JM and BM pastes, respectively.

ences between JM and BM are more pronounced when higher drug loadings (90 wt%, Fig. 5(b)) are processed. The extrusion profile for the JM paste shows a compaction stage prior to the extrusion of the wet mass, most likely due to the different packing properties of the milled materials. The initial extrusion pressure of 90 wt% JM paste (7 MPa) is almost half that of the corresponding 50 wt% loaded formulation (13 MPa), despite the increase in drug loading; this is once again consistent with liquid phase migration occurring during the extrusion, as is also evident from the steady increase in  $P_{ex}$  up to the final value of 33 MPa. In contrast, the BM paste shows a relatively steady flow state throughout the extrusion, after an initial extrusion pressure of ~6 MPa.

**Table 3**

Particle size and shape values for  $\text{CaSO}_4$  and 5-ASA HD.

	Volume basis	$\text{CaSO}_4$		5-ASA HD	
		Laser scattering	Automated microscope	Laser scattering	Automated microscope
Particle size parameter/ $\mu\text{m}$	$d_{10}$	9.5	15.7	10.8	18.7
	$d_{50}$	30.0	54.4	64.2	37.1
	$d_{90}$	107	116	166	64.1
Particle shape parameter	Circularity (mean)	0.63		0.38	
	Aspect ratio (mean)	0.58		0.53	

These results indicate that the particle size and shape of 5-ASA are critical parameters affecting the packing as well as the flow properties of the pastes. On the basis of the different behaviour of JM and BM pastes, we postulate that the shape of the 5-ASA particles, in addition to their size, is a key factor in the extrusion of highly loaded pastes with Avicel PH101 as an extrusion aid at this length scale. In order to confirm this hypothesis, the behaviour of a reference material, having a similar particle morphology to that of 5-ASA, undergoing extrusion was investigated.

### 3.3.2. Influence of needle-like morphology of 5-ASA: control test

The dehydrate (gypsum) polymorph of calcium sulphate (labelled  $\text{CaSO}_4$ ) was selected as a reference material: it is a sparingly soluble material with prolate shaped particles similar to those of 5-ASA. In order to assess the influence of particle shape of the active ingredient on Avicel PH101-based pastes undergoing extrusion, a commercial high density grade of 5-ASA (labelled HD) was also investigated. Particle size/shape characteristics and micrographs of  $\text{CaSO}_4$  and HD are reported in Table 3 and Fig. 6, respectively. Divergences between the laser scattering and the automated microscope as sizing methods were again evident. HD and  $\text{CaSO}_4$  particles are prolate, even though their aspect ratios are different from that of uM crystals (Fig. 3). The uM particles are more tapered whereas HD and  $\text{CaSO}_4$  crystals are more coarse. Moreover, HD particles are slightly more acicular than  $\text{CaSO}_4$  ones, as confirmed by the circularity data in Table 3.

A ram extrusion study, at varying conditions of die length and diameter and extrusion velocity, was performed on Avicel PH101-based pastes containing increasing amounts of active ingredient. Since  $\text{CaSO}_4$  and 5-ASA differ in terms of their solid density values ( $2.32$  and  $1.53 \text{ g cm}^{-3}$ , respectively), pastes were prepared on a volume rather than a weight basis. No sedimentation or segregation effects were observed.

Fig. 7 presents the extrusion pressure–ram displacement profiles for 60 vol% active ingredient/Avicel PH101 pastes. In agreement with the particle shape characteristics, the HD and  $\text{CaSO}_4$  pastes show a similar trend in the extrusion profile to that observed for uM, namely a steady increase in  $P_{ex}$  with ram displacement, indicating that dewatering of pastes is occurring during extrusion. Interestingly, LPM is more pronounced when the HD and  $\text{CaSO}_4$  pastes are extruded, thus suggesting that particle shape, rather than particle size, is the critical parameter in the extrusion of Avicel PH101-based pastes. Both  $\text{CaSO}_4$  and HD pastes yielded over-wet surface extrudates which could not be spheronised.

### 3.4. Influence of alternative MCC grades as E–S aids

The previous section demonstrated the influence of API shape on the extrusion of Avicel PH101/‘hard API’ pastes. The potential influence of the E–S aid was also investigated. The water retention ability, rheology and the performance as an E–S aid of Avicel PH101 for high 5-ASA loadings is now compared to that of two colloidal MCC grades containing NaCMC, namely Avicel RC591 and CL611.



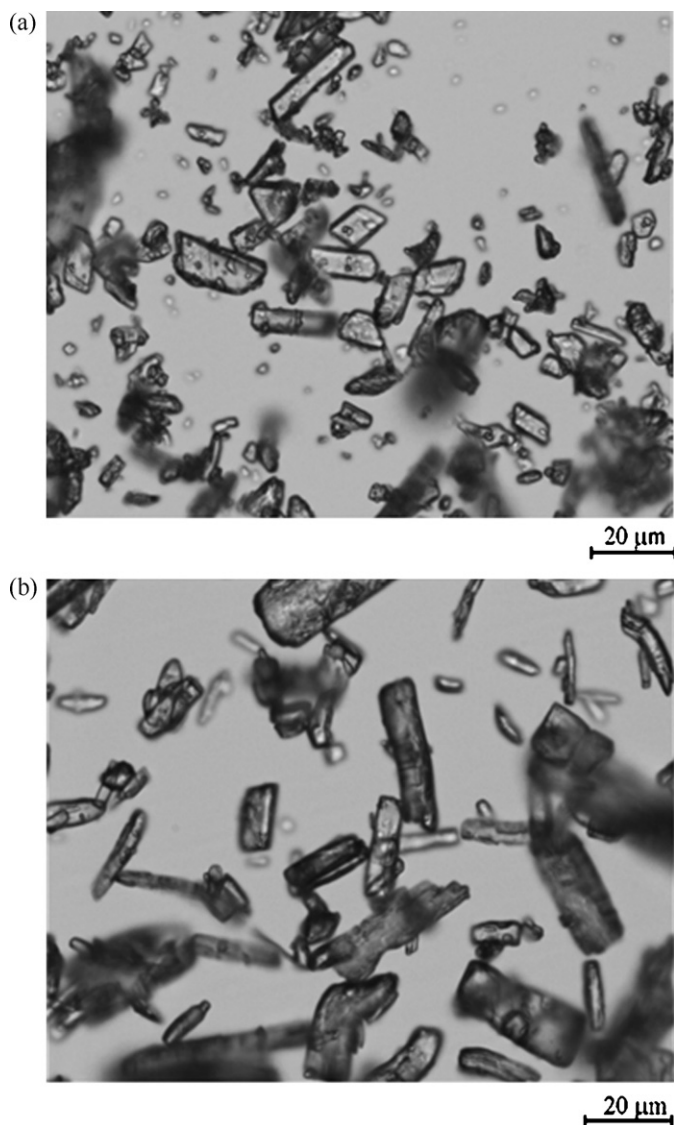


Fig. 6. Micrographs of (a)  $\text{CaSO}_4$  and (b) 5-ASA HD (magnification  $50\times$ ).

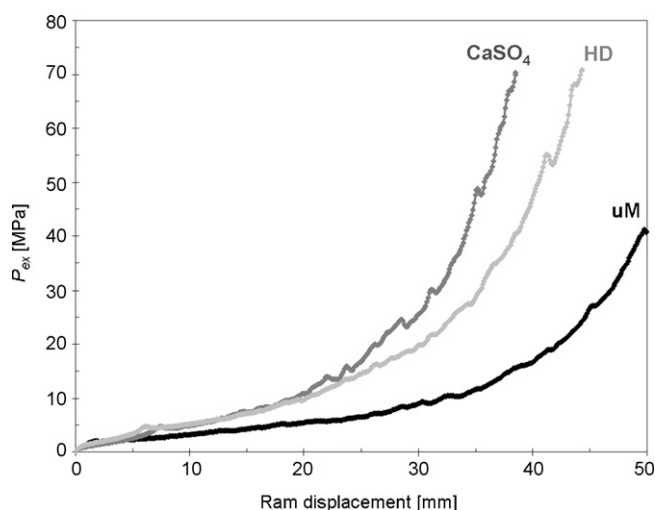


Fig. 7. Extrusion profiles for Avicel PH101-based pastes containing 60 vol% of uM, 5-ASA HD or  $\text{CaSO}_4$  at  $V_{\text{ram}} = 1 \text{ mm s}^{-1}$ , 6-holed die ( $D = 1 \text{ mm}$ ,  $L = 4 \text{ mm}$ ).

### 3.4.1. Centrifuge testing

The water retention ability of the standard MCC and the colloidal grades was assessed by centrifugation, performed on pastes containing different amounts of water. Plots of water/MCC mass ratio vs. centrifugal pressure are presented in Fig. 8. Fig. 8(a) shows that Avicel PH101 is able to retain an amount of water almost equal to its own mass, even after the application of high centrifugal forces. However, for water contents above 50 wt%, the water-holding ability of Avicel PH101 steadily decreases with increasing centrifugal pressure. After being subjected to the highest centrifugal pressure value (180 kPa) for 60 min, all PH101 pastes reached a minimal water/MCC value of about 0.8. This suggests that the water/Avicel PH101 ratio of 1:1.2 might represent the maximum water quantity that the microcrystalline fibrils are able to retain within their internal structure. Once this saturation level is reached, additional water would be loosely associated in the free space between the cellulose particles and therefore readily lost during centrifugation. Extended centrifuge testing over 120 min (data not shown) gave similar results to those performed at 60 min. Fig. 8(b) and (c) shows that both the colloidal MCC grades are able to retain more than twice their own mass of water even when subjected to the highest centrifugal pressures. A plot of percentage water loss against initial paste water content for the three MCC grades (Fig. 8(d)), at 180 kPa centrifugal pressure, also gives an indication of the water-retaining ability of the pastes. In order to validate the efficiency of the centrifuge testing, a control study using inert glass spheres (ballotini) having a particle size similar to that of MCC was performed (data not shown). As expected, the water added to the ballotini 'paste' was completely drained after the centrifuge run. The greater water-retaining ability of the colloidal MCC grades was further confirmed by ram extrusion testing.

### 3.4.2. Ram extrusion studies

**3.4.2.1. MCC pastes.** The rheological behaviour and the water retention ability of the standard PH101 grade of MCC were compared to that of the modified RC591 and CL611 grades. Ram extrusion testing was performed using a square-entry single-holed capillary die ( $D = 2 \text{ mm}$ ,  $L = 2 \text{ mm}$ ) over a ram displacement of 100 mm, on 50, 55, 60 and 65 wt% water/MCC pastes, at  $V_{\text{ram}}$  speeds of 0.1, 1 and  $10 \text{ mm s}^{-1}$ .

Table 4 lists the average  $P_{\text{ex}}$  values for the formulations tested. For those formulations which exhibited LPM, initial and final  $P_{\text{ex}}$  values, marked by an asterisk, are reported. As expected, for a given MCC grade, the extrusion pressure increases with increasing  $V_{\text{ram}}$ , and decreases with increasing water content.

All PH101 pastes exhibited liquid phase migration at the lowest ( $0.1 \text{ mm s}^{-1}$ ) and intermediate ( $1 \text{ mm s}^{-1}$ ) ram velocities, whereas at the highest  $V_{\text{ram}}$  ( $10 \text{ mm s}^{-1}$ ) LPM was observed only for the 65 wt% water/PH101 formulation. Avicel RC591 only showed some LPM at  $V_{\text{ram}} = 0.1 \text{ mm s}^{-1}$ , while the intensity of dewatering for RC591 pastes (profiles not shown) was always less pronounced than that observed for the corresponding PH101 pastes. LPM was not observed with Avicel CL611, and smooth extrusion profiles were obtained at all combinations of  $V_{\text{ram}}$  and water content investigated. By way of example, Fig. 9 presents  $P_{\text{ex}}$  profiles for 50 wt% water/MCC pastes performed at  $V_{\text{ram}} = 1 \text{ mm s}^{-1}$ .

The ram extrusion study, in agreement with the centrifuge results, demonstrates the improved ability of colloidal MCC grades to hinder water migration when subjected to pressure.

**3.4.2.2. Colloidal MCC/5-ASA pastes.** RC591 and CL611 grades of MCC were investigated as alternative E-S aids to Avicel PH101 in 5-ASA based pastes. The amount of water used for paste preparation was selected on the basis of the centrifuge testing. Since colloidal MCC grades have a greater water-retaining ability than the



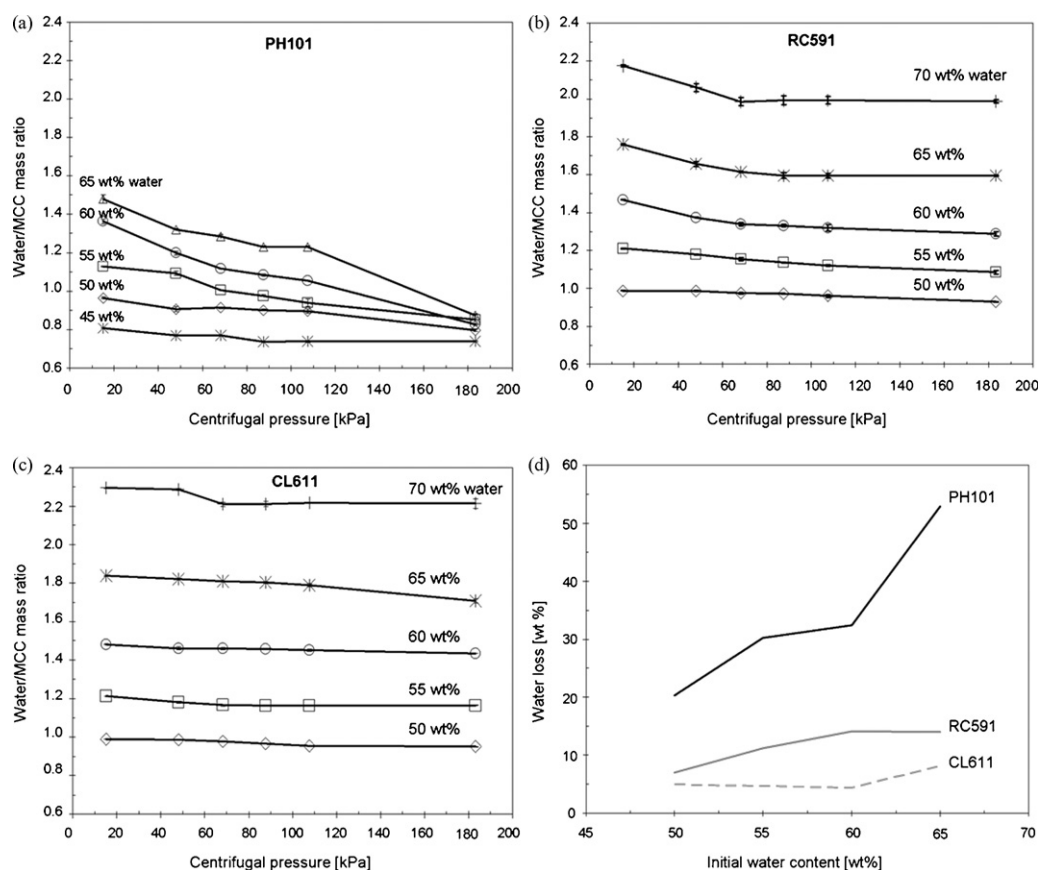


**Fig. 8.** Water/MCC mass ratio vs. centrifugal pressure profiles for Avicel (a) PH101, (b) RC591 and (c) CL611; (d) water loss profiles of MCC pastes at 180 kPa centrifugal pressure.

standard PH101, the amount of water necessary to obtain a plastic mass suitable for extrusion was greater. The water/colloidal MCC mass ratio selected was 1.5:1; both a wet mass and extrudates with appropriate characteristics of plasticity could be obtained with this amount of water.

Fig. 10(a) shows an example of the  $P_{ex}$ –ram displacement profiles obtained for 50 wt% uM/MCC pastes. By replacing the standard MCC grade with the colloidal ones, LPM was reduced or eliminated. In contrast to the Avicel PH101 based paste,  $P_{ex}$  for the colloidal grades of MCC reached steady state shortly after extrusion started, indicating that little dewatering occurred. This was confirmed by monitoring the water content distribution of both the extrudate during ram extrusion and the remaining billet within the barrel

(see Fig. 10(b)). The Avicel PH101 based formulation showed a relatively large difference in extrudate water content from that of the initial paste. This is manifested as an over-wet extrudate and a relatively dry paste billet in the barrel. On the contrary, the water content of the extrudate and the billet for both the colloidal MCC grades is close to the initial value, thereby indicating that the water was strongly held within the MCC–NaCMC fibril network.

The extrudates obtained were subjected to spheronisation: both RC591 and CL611 based formulations yielded spherical granules, whereas PH101 failed, yielding over-wet extrudates that aggregated during spheronisation.

The behaviour of these colloidal MCC grades with high loadings of 5-ASA (*i.e.* 90 wt%) was also assessed. Fig. 11 presents the extru-

**Table 4**

Average  $P_{ex}$  values for MCC/water pastes at  $V_{ram} = 0.1, 1$  and  $10 \text{ mm s}^{-1}$ , single-holed capillary die ( $D = 2 \text{ mm}$ ,  $L = 2 \text{ mm}$ ). Asterisk values indicate LPM: initial and final extrusion pressures are reported for a ram displacement of 100 mm. Coefficient of variation (CV, %) given in parentheses.

wt% water	$V_{ram}/\text{mm s}^{-1}$	$P_{ex}/\text{MPa}$ (CV, %)		
		PH101	RC591	CL611
50	0.1	2.31–11.2* (51.3)	7.75 (6.29)	2.76 (2.97)
	1	4.68–7.27* (14.3)	4.81 (2.32)	3.49 (2.11)
	10	7.11 (5.45)	7.76 (6.24)	5.19 (7.14)
55	0.1	0.797–2.86* (9.87)	2.30 (9.87)	1.47 (2.11)
	1	1.63–2.27* (15.9)	2.30 (9.87)	1.88 (1.73)
	10	2.86 (5.11)	3.67 (1.83)	2.90 (3.66)
60	0.1	0.532–0.925* (18.2)	0.532–0.922* (10.10)	0.717 (7.02)
	1	0.800–1.15* (13.4)	0.715 (7.86)	0.924 (2.75)
	10	1.25 (6.45)	1.77 (1.92)	1.49 (4.30)
65	0.1	0.076–0.213* (34.5)	0.323–0.567* (14.2)	0.369 (5.58)
	1	0.090–0.207* (20.1)	0.545 (5.09)	0.568 (1.36)
	10	0.155–0.315* (25.1)	0.797 (6.97)	0.919 (2.77)

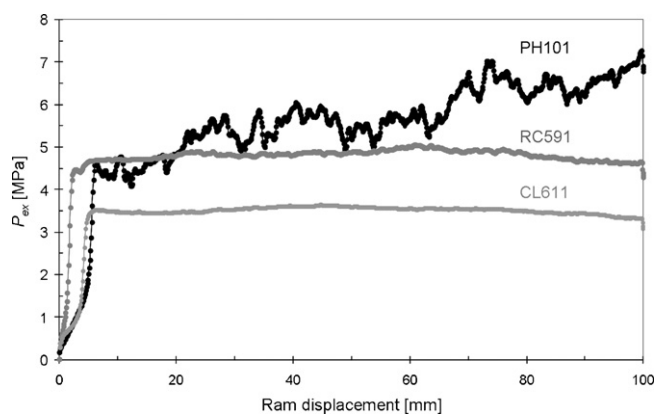


**Fig. 9.** Extrusion profiles for 50 wt% water/MCC (Avicel PH101, RC591 and CL611) pastes at  $V_{ram} = 1 \text{ mm s}^{-1}$ , single-holed capillary die ( $D = 2 \text{ mm}$ ,  $L = 2 \text{ mm}$ ).

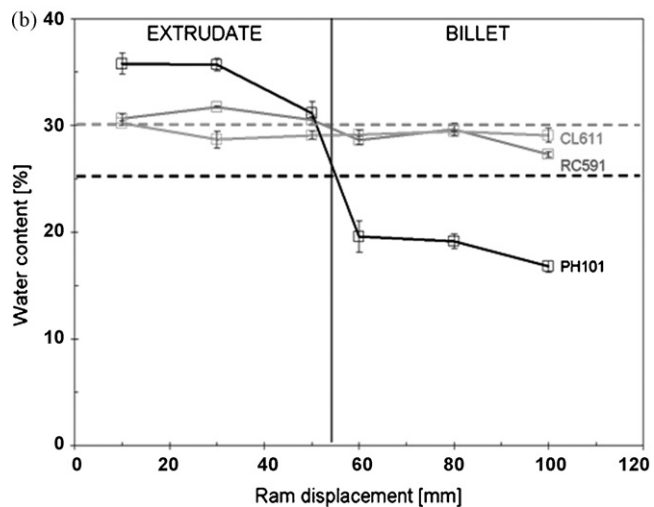
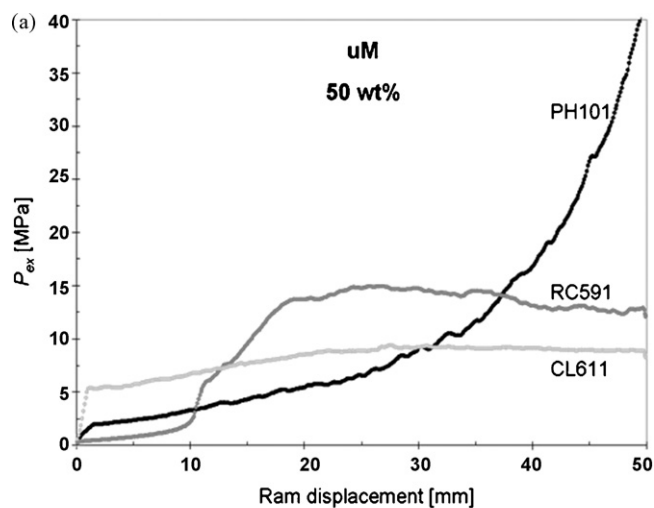


**Fig. 10.** (a) Extrusion profiles for 50 wt% uM/MCC (Avicel PH101, RC591 and CL611) pastes at  $V_{ram} = 1 \text{ mm s}^{-1}$ , 6-holed die ( $D = 1 \text{ mm}$ ,  $L = 4 \text{ mm}$ ) and (b) water content profile of extrudates throughout ram extrusion and the remaining paste billet. Horizontal lines in (b) indicate initial paste water content of colloidal MCCs (grey) and Avicel PH101 (black). Error bars indicate standard error (3 replicates).

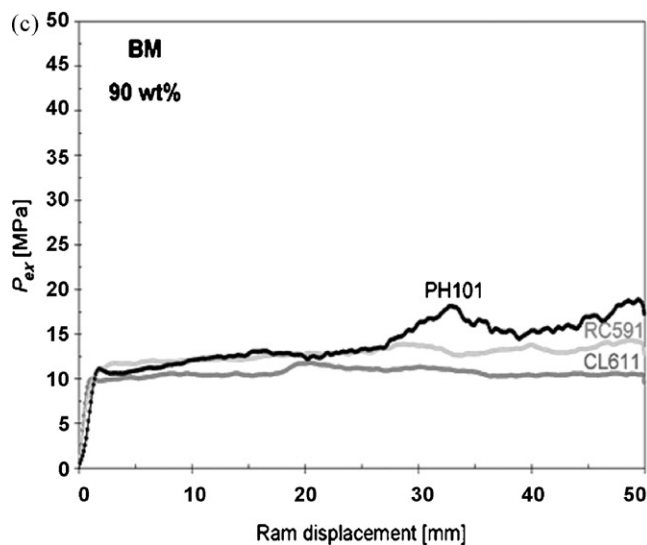
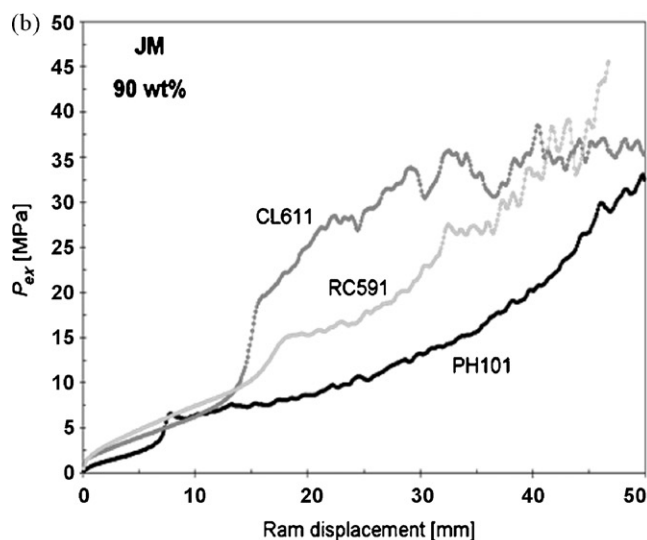
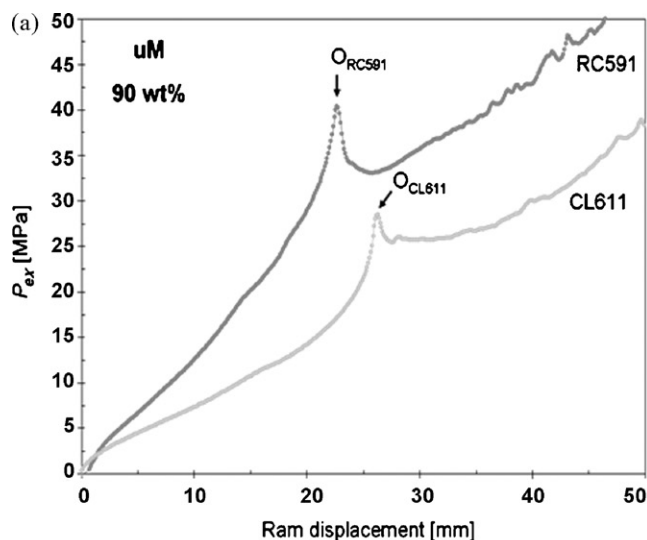


**Fig. 11.** Extrusion profiles for MCC-based pastes containing 90 wt% of (a) uM, (b) JM and (c) BM at  $V_{ram} = 1 \text{ mm s}^{-1}$ , 6-holed die ( $D = 1 \text{ mm}$ ,  $L = 4 \text{ mm}$ ). Points labelled  $O_{RC591}$ ,  $O_{CL611}$  and  $O_{PH101}$  in (a) and (c) indicate the onset of extrusion for Avicel RC591, CL611 and PH101 pastes, respectively.

sion profiles obtained for 90 wt% API loaded pastes with uM, JM and BM. Both the colloidal MCC grades allowed a 90 wt% uM loaded formulation to be extruded (Fig. 11(a)), whereas Avicel PH101 failed (see Section 3.3.1). However, both uM/RC591 and uM/CL611 started extruding at relatively high values of  $P_{ex}$  (41 and 28 MPa, respectively), after an extended compaction stage coupled with severe liquid phase migration throughout the extrusion. Analogously, JM pastes (Fig. 11(b)) showed a similar extrusion trend, even though the overall  $P_{ex}$  values are slightly lower. Conversely, BM-based pastes (Fig. 11(c)) gave steady extrusion profiles, following the onset of extrusion (occurring at 10 MPa for the CL611-based paste and at  $\sim 11$  MPa for the PH101 and RC591 ones). The importance of particle shape, rather than particle size of 5-ASA in the extrusion process of MCC based pastes, is once again confirmed.

Previous workers, e.g. Harrison et al. (1985), demonstrated that steady-state flow during the extrusion process is necessary to obtain good quality extrudates (i.e. ones with a smooth surface); this was confirmed in the current study. However, good quality extrudate does not always imply its suitability for spheronisation. In fact BM/PH101 pastes yielded good quality (without surface defects) extrudates, but these were not able to give satisfactory spheres when subjected to spheronisation; the extrudates obtained did not have sufficient plasticity either to break up or to be rounded off within the spheroniser (Fig. 12(a)). However, increasing the moisture content in the paste formulation, to enhance plasticity, led to over wet-surface extrudates and resulted in uncontrollable agglomeration. Conversely, both BM/RC591 and BM/CL611 pastes exhibited steady extrusion profiles and furthermore yielded extru-

dates that were able to be broken up in the spheroniser and to form satisfactory spheres (Fig. 12(b)).

The overall results indicate that particle size and shape of the API (and thereby an appropriate process of milling) are important parameters to be taken into account when high drug loadings need to be processed by extrusion–spheronisation. Analogously, the E–S aid type used is also an important issue to be considered, as it can determine the feasibility of the spheronisation process and/or the characteristics of the final product. The influence of process parameters (e.g. spheronisation time and speed) on the properties of the final pellets will be investigated further.

#### 4. Conclusions

The feasibility of an E–S route for the manufacture of highly loaded 5-ASA multiparticulate dosage forms was assessed. The influence of the API chemical and physical properties on the rheological behaviour of MCC-based pastes undergoing extrusion was investigated. Two batches of micronised 5-ASA, with different particle size and shape characteristics, were prepared and their extrusion behaviour was compared to that of the starting material. The performance as E–S aids of the standard Avicel PH101 grade of MCC and of colloidal ones (i.e. Avicel RC591 and CL611), alongside high loadings of 5-ASA, was also evaluated. Centrifugation testing, supported by ram extrusion studies, was used to establish the water retention ability of paste materials and to determine the minimal water content required to obtain a wet mass with an appropriate degree of plasticity for extrusion and spheronisation.

Acute liquid phase migration (LPM), resulting in a non-uniform distribution of water within the extrudates, was generally observed for the 5-ASA/Avicel PH101 paste formulations. This was demonstrated to be dependent on both the drug loading and the type of extrusion aid. Drug particle morphology (needle-like) was identified as the critical parameter, which was confirmed by extruding calcium sulphate/MCC pastes, where the sulphate polymorph was selected to match the 5-ASA shape. A reduction in particle size, combined with a change in particle morphology, allowed LPM to be considerably reduced or eliminated. The effect of pH on MCC behaviour was found to be negligible. Colloidal grades of MCC were identified to be promising alternatives to the standard PH101 in extrusion of high 5-ASA loadings, due to their ability to hinder water migration when subjected to pressure. Based on the results obtained, a multiparticulate E–S formulation containing not less than 90 wt% 5-ASA could be developed by combining an accordingly micronised API and colloidal MCC grade.

#### Acknowledgements

The authors wish to thank IMS Micronizzazioni S.p.A. (Milano, Italy) for providing the air-jet milled batch of 5-ASA. The microcrystalline cellulose was kindly provided by IMCD S.p.A. (San Donato Milanese, Italy). The assistance of Mr. Z. Saracevic (Department of Chemical Engineering and Biotechnology, University of Cambridge) is gratefully acknowledged.

#### References

- Allgayer, H., Sonnenbichler, J., Kruis, W., Paumgartner, G., 1985. Determination of the pK values of 5-aminosalicylic acid and N-acetylaminosalicylic acid and comparison of the pH dependent lipid–water partition coefficients of sulphasalazine and its metabolites. *Arzneimittelforschung* 35, 1457–1459.
- Bechgaard, H., Hagermann, N.G., 1978. Controlled-release multi-units and single unit doses. A literature review. *Drug Dev. Ind. Pharm.* 4, 53–67.
- Bains, D., Boutell, S.L., Newton, J.M., 1991. The influence of moisture content on the preparation of spherical granules of barium sulphate and microcrystalline cellulose. *Int. J. Pharm.* 69, 233–237.

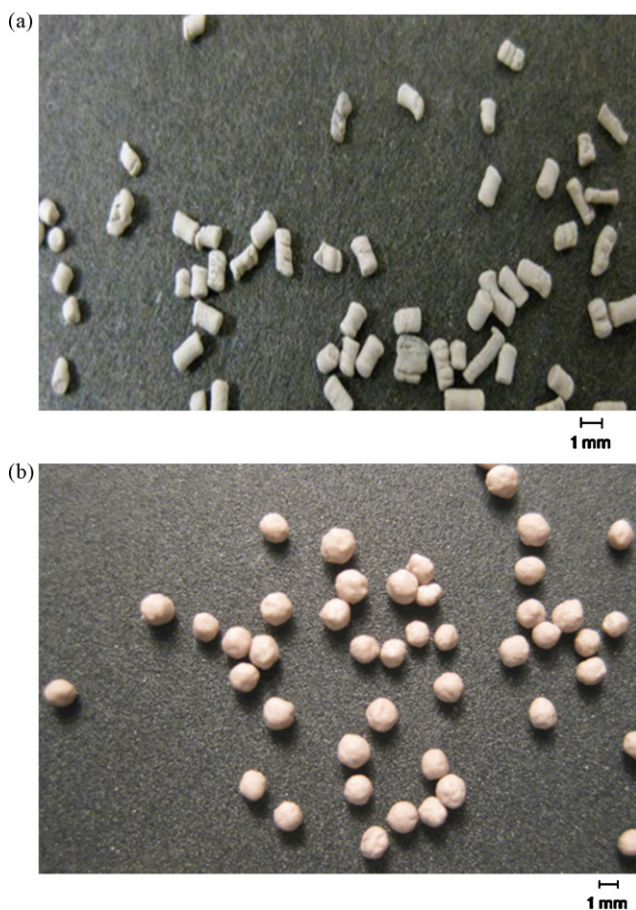


**Fig. 12.** Micrographs of dried pellets containing 90 wt% BM and 10 wt% (a) Avicel PH101 and (b) CL611. Extrusion: 6-holed die ( $D = 1$  mm,  $L = 4$  mm);  $V_{ram} = 1$  mm s<sup>-1</sup>. Spheronisation: 10 min; 1600 rpm.

- Buckland, A., Bodger, K., 2008. The cost-utility of high dose oral mesalazine for moderately active ulcerative colitis. *Aliment. Pharmacol. Ther.* 28, 1287–1296.
- Cervený, P., Bortlík, M., Kubena, A., Vlcek, J., Lakatos, P.L., Lukás, M., 2007. Nonadherence in inflammatory bowel disease: results of factor analysis. *Inflamm. Bowel Dis.* 13, 1244–1249.
- Chuong, M.C., Christensen, J.M., Ayres, J.W., 2008. Sustained delivery of intact drug to the colon: mesalamine formulation and temporal gastrointestinal transit analysis. *Pharm. Dev. Technol.* iFirst, 1–10, doi:10.1080/10837450802420559.
- Cohen, R.D., 2006. Review article: evolutionary advances in the delivery of aminosaliculates for the treatment of ulcerative colitis. *Aliment. Pharmacol. Ther.* 24, 465–474.
- Fielden, K.E., Newton, J.M., O'Brien, P., Rowe, R.C., 1988. Thermal studies on the interaction of water and microcrystalline cellulose. *J. Pharm. Pharmacol.* 40, 674–678.
- Fielden, K.E., Newton, J.M., Rowe, R.C., 1992. The influence of lactose particle size on spheronization of extrudate processed by a ram extruder. *Int. J. Pharm.* 81, 205–224.
- Gazzaniga, A., Sangalli, M.E., Bruni, G., Zema, L., Vecchio, C., Giordano, F., 1998. The use of  $\beta$ -cyclodextrin as a pelletization agent in the extrusion/spheronization process. *Drug Dev. Ind. Pharm.* 24, 869–873.
- Goskonda, S.R., Hileman, G.A., Upadrashta, S.M., 1994. Development of matrix controlled release beads by extrusion–spheronization technology using a statistical screening design. *Drug Dev. Ind. Pharm.* 20, 279–292.
- Hagsten, A., Casper Larsen, C., Møller Sonnergaard, J., Rantanen, J., Hovgaard, L., 2008. Identifying sources of batch to batch variation in processability. *Powder Technol.* 183, 213–219.
- Harrison, P.J., Newton, J.M., Rowe, R.C., 1985. The characterisation of wet powder masses suitable for extrusion/spheronisation. *J. Pharm. Pharmacol.* 37, 686–691.
- Hassler, G.L., Brunner, E., 1945. Measurement of capillary pressures in small core samples. *Trans. AIME* 160, 114–123.
- Hileman, G.A., Goskonda, S.R., Spalitto, A.J., Upadrashta, S.M., 1993. A factorial approach to high dose product development by an extrusion/spheronization process. *Drug Dev. Ind. Pharm.* 19, 483–491.
- Kraeger, J.S., Edge, S., Price, R., 2004. Influence of particle size and shape on flowability and compactibility of binary mixtures of paracetamol and microcrystalline cellulose. *Eur. J. Pharm. Sci.* 22, 173–179.
- Krieger, M., Dougherty, J., 1959. A mechanism for non-Newtonian flow in suspensions of rigid spheres. *J. Rheol.* 3, 137–152.
- Latimer, P., Brunsting, A., Pyle, B.E., Moore, C., 1978. Effects of asphericity on single particle scattering. *Appl. Opt.* 17, 3152–3158.
- Mascia, S., Patel, M.J., Rough, S.L., Martin, P.J., Wilson, D.I., 2006. Liquid phase migration in the extrusion and squeezing of microcrystalline cellulose pastes. *Eur. J. Pharm. Sci.* 29, 22–34.
- O'Connor, R.E., Holinej, J., Schwartz, J.B., 1984. Spheronization I: processing and evaluation of spheres prepared from commercially available excipients. *Am. J. Pharm.* 156, 80–87.
- Podczek, F., Knight, P., 2006. The evaluation of formulations for the preparation of pellets with high drug loading by extrusion/spheronization. *Pharm. Dev. Technol.* 11, 263–274.
- Podczek, F., Knight, P.E., Newton, J.M., 2007. The evaluation of modified microcrystalline cellulose for the preparation of pellets with high drug loading by extrusion/spheronization. *Int. J. Pharm.* 350, 145–154.
- Rough, S.L., Bridgwater, J., Wilson, D.I., 2000. Effects of liquid phase migration on extrusion of microcrystalline cellulose pastes. *Int. J. Pharm.* 204, 117–126.
- Rough, S.L., Wilson, D.I., Bridgwater, J., 2002. A model describing liquid phase migration within an extruding microcrystalline cellulose paste. *Chem. Eng. Res. Des.* 80, 701–714.
- Rough, S.L., Wilson, D.I., 2005. Extrudate fracture and spheronisation of microcrystalline cellulose pastes. *J. Mater. Sci.* 40, 4199–4219.
- Rudolph, M.W., Klein, S., Beckert, T.E., Peterleit, H.-U., Dressman, J.B., 2001. A new 5-aminosalicylic acid multi-unit dosage form for the therapy of ulcerative colitis. *Eur. J. Pharm. Biopharm.* 51, 183–190.
- Tomer, G., Podczek, F., Newton, J.M., 2001. The influence of type and quantity of model drug on the extrusion/spheronization of mixtures with microcrystalline cellulose. I: Extrusion parameters. *Int. J. Pharm.* 217, 237–248.
- Tomer, G., Podczek, F., Newton, J.M., 2002. The influence of model drugs on the preparation of pellets by extrusion/spheronization. II: Spheronization parameters. *Int. J. Pharm.* 231, 107–119.
- Vervaeke, C., Baert, L., Remon, J.P., 1995. Extrusion–spheronisation. A literature review. *Int. J. Pharm.* 116, 131–146.
- Wei, H.E., Fan, L.-F., Min, B., Yong-Zhen, C., Bai S X., Qing, D., Feng, W., Min, Q., De-Ying, C., 2010. Chitosan/kollicoat SR 30D film-coated pellets of aminosaliculates for colonic drug delivery. *J. Pharm. Sci.* 99, 186–195.